

## **ON THE OXIDATION BEHAVIOUR OF MONOLITHIC TiB<sub>2</sub> AND Al<sub>2</sub>O<sub>3</sub>-TiB<sub>2</sub> AND Si<sub>3</sub>N<sub>4</sub>-TiB<sub>2</sub> COMPOSITES**

*A. Tampieri, E. Landi and A. Bellosi*

CNR-IRTEC, RESEARCH INSTITUTE FOR CERAMICS TECHNOLOGY, FAENZA, ITALY

In view of the susceptibility of TiB<sub>2</sub> to oxidation, the thermal stability of monolithic TiB<sub>2</sub> and of Al<sub>2</sub>O<sub>3</sub>-30 vol% TiB<sub>2</sub> and Si<sub>3</sub>N<sub>4</sub>-20 vol% TiB<sub>2</sub> composites was investigated. The temperature at which TiB<sub>2</sub> ceramic starts to oxidize is about 400°C, oxidation kinetics being controlled by diffusion up to  $T \approx 900^\circ\text{C}$  and in the first stage of the oxidation at 1000°C and 1100°C (up to 800 min and 500 min respectively), and by a linear law at higher temperatures and for longer periods.

Weight gains in the Al<sub>2</sub>O<sub>3</sub>-TiB<sub>2</sub> composite can be detected only at temperatures above  $\approx 700^\circ\text{C}$  and the rate governing step of the oxidation reaction is characterized by a one-dimensional diffusion mechanism at  $T = 700^\circ\text{C}$  and  $T = 800^\circ\text{C}$  and by two-dimensional diffusion at higher temperatures.

Concerning the Si<sub>3</sub>N<sub>4</sub>-TiB<sub>2</sub> composite, three different oxidation behaviours related to the temperature were observed, i.e. up to  $\approx 1000^\circ\text{C}$  the reaction detected regards only the second phase; at  $\approx 1000 < T < \approx 1200^\circ\text{C}$ , the diffusion of O<sub>2</sub> or N<sub>2</sub> through an oxide layer is proposed as the rate-governing step; at  $T > \approx 1200^\circ\text{C}$ , a linear kinetic indicates the formation of a non protective scale.

**Keywords:** monolithic TiB<sub>2</sub> and Al<sub>2</sub>O<sub>3</sub>-TiB<sub>2</sub> and Si<sub>3</sub>N<sub>4</sub>-TiB<sub>2</sub> composites, oxidation kinetics

### **Introduction**

Titanium diboride has been studied extensively for its potential applications and it has received great attention because of its high melting point, hardness, electrical conductivity and wettability by molten Al [1-3].

The addition of TiB<sub>2</sub> to an Al<sub>2</sub>O<sub>3</sub> or Si<sub>3</sub>N<sub>4</sub> matrix greatly increases hardness, strength and fracture toughness; in addition, these composites can be used as electrodes, wear parts, cutting tools, high temperature heaters and heat exchangers.

*John Wiley & Sons, Limited, Chichester  
Akadémiai Kiadó, Budapest*

In this respect the thermal stability of monolithic  $\text{TiB}_2$ , of  $\text{Al}_2\text{O}_3$ - $\text{TiB}_2$  and  $\text{Si}_3\text{N}_4$ - $\text{TiB}_2$  composites is an important property to evaluate, since in use they can be exposed to oxidizing environments.

Moreover, because of the propensity of titanium diboride to oxidize, the success of the composites in high temperature applications will depend on the extent to which the matrix can prevent the oxidation of  $\text{TiB}_2$  particles [7–9].

The purpose of this study is to evaluate the thermal stability in air of  $\text{TiB}_2$  and of oxide ( $\text{Al}_2\text{O}_3$ )- and non-oxide ( $\text{Si}_3\text{N}_4$ )-based composites containing  $\text{TiB}_2$  as a secondary phase.

Thermal oxidation causes a net-weight gain which can be monitored using thermogravimetric analysis to determine the oxidation kinetics. On the basis of the morphological and structural characteristics of the oxidized surfaces and of the kinetic and thermodynamic parameters, an evaluation of the phenomenological processes involved was attempted.

## Experimental procedure

### *Materials*

Starting with a commercial  $\text{TiB}_2$  powder (Starck, Grade F), dense  $\text{TiB}_2$  ceramics were obtained through hot pressing at  $1850^\circ\text{C}$  for 60 min and at 30 MPa [3].

$\text{Al}_2\text{O}_3$ - $\text{TiB}_2$  composites were produced by adding 30 vol%  $\text{TiB}_2$  to  $\text{Al}_2\text{O}_3$  (Alcoa A16 S. G.) and by hot pressing the mixture at  $1600^\circ\text{C}$ , 30 MPa for 30 min [10].

With regards to the  $\text{Si}_3\text{N}_4$  composite, silicon nitride powders (Starck LC12) were wet mixed with the sintering aids (3 wt%  $\text{Al}_2\text{O}_3$  and 8 wt%  $\text{Y}_2\text{O}_3$ ) and then  $\text{TiB}_2$  in 20 vol% amount was added. Dense samples were obtained by uniaxially hot pressing at  $1750^\circ\text{C}$  and 30 MPa.

Starting compositions, hot pressing conditions, the values of some microstructural parameters and mechanical properties of monolithic  $\text{TiB}_2$  and of the composites have been reported elsewhere [3, 6, 10].

### *Oxidation tests*

Short term oxidation tests (20–30 hours) were carried out in a static air atmosphere on samples diamond sawn from the hot pressed billets, then polished and cleaned. The weight gains were continuously recorded by a TG-DTA apparatus (P. L. Thermal Sciences, U. K.); oxidation temperatures ranged from  $350^\circ$  to  $1400^\circ\text{C}$ ; the heating rate was  $30 \text{ deg}\cdot\text{min}^{-1}$ .

The surface of the oxidized samples was analyzed by X-ray Diffraction (Rigaku Corporation), Scanning Electron Microscopy (Autoscan, ETEC, USA),

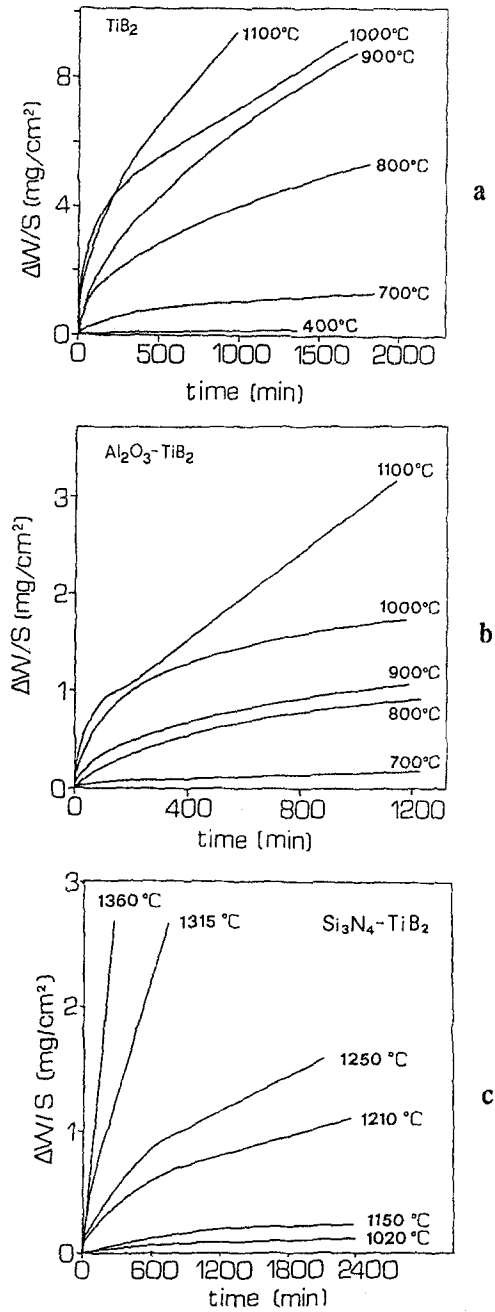


Fig. 1 Isothermal weight gain at various temperatures for: a)  $\text{TiB}_2$ ; b)  $\text{Al}_2\text{O}_3\text{-TiB}_2$ ; c)  $\text{Si}_3\text{N}_4\text{-TiB}_2$

including Back-scattered electron imaging and Energy-Dispersive Spectroscopy (Philips, EDAX PV 9100).

## Results and discussion

Under isothermal conditions, weight gains (DW/S, where DW is the weight gain and S is the surface of the sample) were detected starting at about 400°C for TiB<sub>2</sub> (Fig. 1a), at about 700°C for Al<sub>2</sub>O<sub>3</sub>-TiB<sub>2</sub> (Fig. 1b) and at about 800°C for Si<sub>3</sub>N<sub>4</sub>-TiB<sub>2</sub> (Fig. 1c).

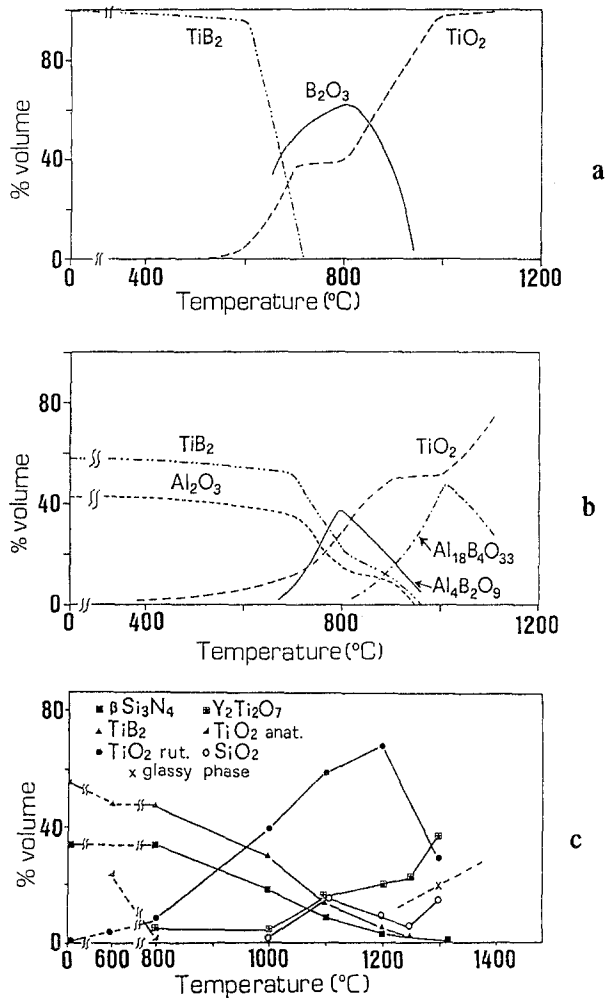
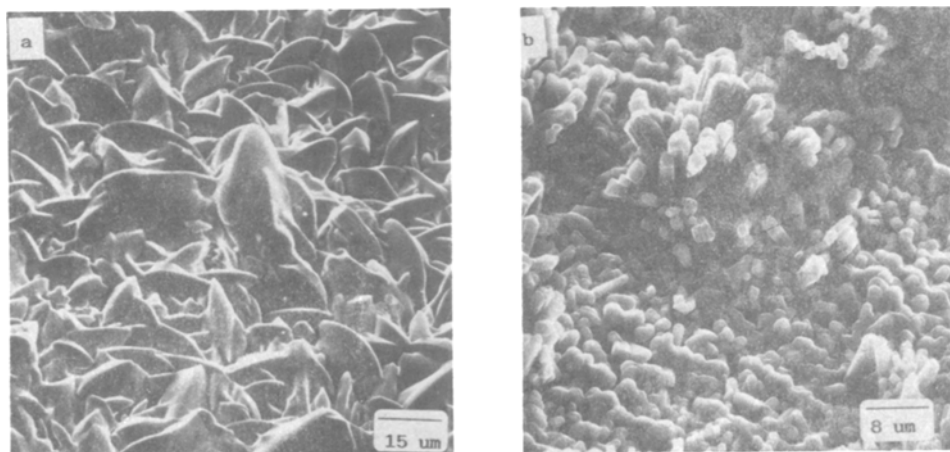


Fig. 2 Semiquantitative X-ray analysis of the oxidized surfaces showing the crystal phase content: a) TiB<sub>2</sub>; b) Al<sub>2</sub>O<sub>3</sub>-TiB<sub>2</sub>; c) Si<sub>3</sub>N<sub>4</sub>-TiB<sub>2</sub>

*a) Structure and morphology of the oxidized surfaces*

The evolution of the crystalline phases content for the oxidized samples as derived from semiquantitative XRD analysis are shown in Fig. 2a, b, c for TiB<sub>2</sub>, Al<sub>2</sub>O<sub>3</sub>-TiB<sub>2</sub> and Si<sub>3</sub>N<sub>4</sub>-TiB<sub>2</sub> respectively. The presence of crystalline TiO<sub>2</sub> was detected at temperatures higher than ≈700°C in Al<sub>2</sub>O<sub>3</sub>-TiB<sub>2</sub> and ≈400°C in TiB<sub>2</sub>. The oxide scale in monolithic TiB<sub>2</sub> samples is also formed by crystalline B<sub>2</sub>O<sub>3</sub> at  $T = 700^{\circ}\text{--}800^{\circ}\text{C}$ . However at  $T > \approx 800^{\circ}\text{C}$  only highly textured TiO<sub>2</sub> crystals are detectable (Fig. 2a). The morphology of the crystals are shown in Fig. 3a.



**Fig. 3** Microstructure of the oxidized surfaces at 1000°C of: a) TiB<sub>2</sub>; b) Al<sub>2</sub>O<sub>3</sub>-TiB<sub>2</sub>

On the oxidized surface of Al<sub>2</sub>O<sub>3</sub>-TiB<sub>2</sub>, the amount of rutile rapidly increases at  $T > 700^{\circ}\text{C}$ . Moreover two aluminium borate phases: Al<sub>4</sub>B<sub>2</sub>O<sub>9</sub> at  $700^{\circ}\text{C} \leq T \leq 900^{\circ}\text{C}$  and Al<sub>18</sub>B<sub>4</sub>O<sub>33</sub> at  $T > 900^{\circ}\text{C}$ , were observed in Al<sub>2</sub>O<sub>3</sub>-TiB<sub>2</sub> (Fig. 2b). Figure 3b shows the microstructure of the Al<sub>2</sub>O<sub>3</sub>-TiB<sub>2</sub> oxidized surface at 1000°C characterized by TiO<sub>2</sub> crystals forming a thick oxide scale.

In the silicon nitride-based composites, up to ≈ 1000°C only the second phase undergoes an oxidation reaction and certain amount of rutile is observed at  $T \geq 700^{\circ}\text{C}$ . At  $T > \approx 1000^{\circ}\text{C}$ , where the Si<sub>3</sub>N<sub>4</sub> matrix is also involved in the oxidation reaction producing mainly SiO<sub>2</sub> and yttrium silicates, some reactions take place on the oxide scale among SiO<sub>2</sub>, TiO<sub>2</sub> and Y-silicates. These reactions produce on the oxide scale after cooling the formation of Y<sub>2</sub>Ti<sub>2</sub>O<sub>7</sub>, glassy silicate phase, crystalline SiO<sub>2</sub> and TiO<sub>2</sub>. Figures 4–6 show the evolution of the surface morphology with the oxidation temperature.

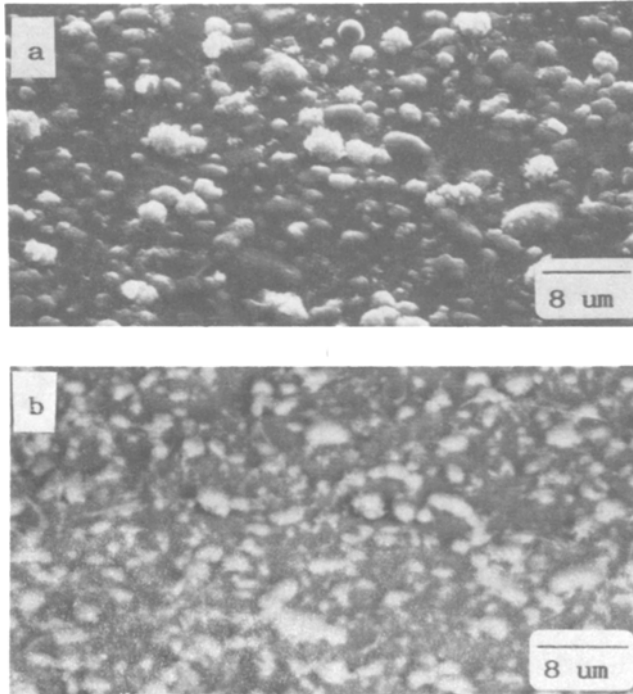
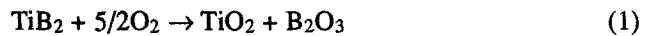


**Fig. 4** Microstructure of the surfaces of  $\text{Si}_3\text{N}_4\text{-TiB}_2$  oxidized at  $820^\circ\text{C}$ : *a*) morphology; *b*) back-scattered electron image

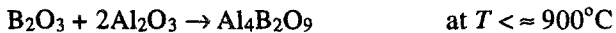
*b) Oxidation kinetics and mechanisms*

It is well known that  $\text{TiB}_2$  oxidizes according to the chemical reaction:

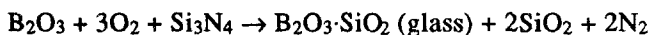


Crystalline  $\text{B}_2\text{O}_3$  has been observed in monolithic  $\text{TiB}_2$  after oxidation at  $T = 700^\circ\text{C}$  and  $T = 800^\circ\text{C}$ .

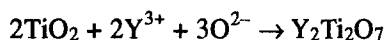
In  $\text{Al}_2\text{O}_3\text{-TiB}_2$ , following the reaction (1), further reactions occur:



In  $\text{Si}_3\text{N}_4\text{-TiB}_2$  composites, the main chemical reactions involved (following reaction 1) are:



minor reaction:



### Monolithic $\text{TiB}_2$

The set of curves in Fig. 1a may be fitted using two kinetic models:

1) diffusion-controlled kinetics  $(DW/S)^2 = kt$ , where  $k$  is the oxidation rate constant, valid up to  $T \approx 900^\circ\text{C}$  for the entire isothermal run; at  $1000^\circ\text{C}$  up to about 800 min, and at  $1100^\circ\text{C}$  up to  $\approx 500$  min;

2) linear behaviour ( $DW/S \approx kt$ ) for longer periods at  $1000^\circ\text{C}$  and  $1100^\circ\text{C}$ . In this case the large volume expansion that occurs during the reaction  $\text{TiB}_2 \rightarrow \text{TiO}_2$  may cause cracking on the oxide layer, resulting in an increase in the active area for oxidation and in a heterogeneous diffusion in the barrier layer.

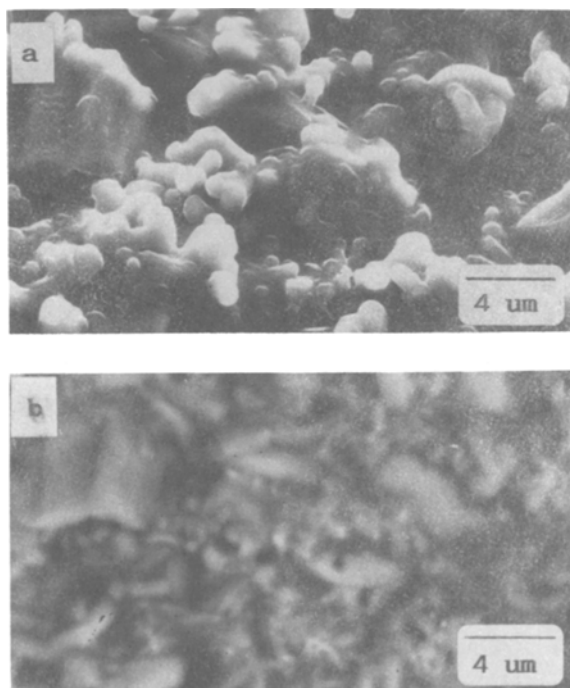
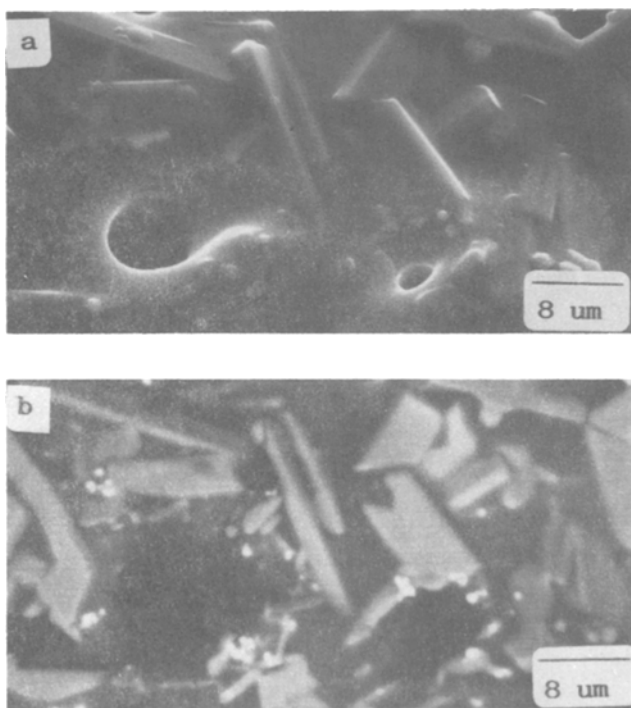


Fig. 5 Microstructure of the surfaces of  $\text{Si}_3\text{N}_4\text{-TiB}_2$  oxidized at  $1020^\circ\text{C}$ : a) morphology; b) back-scattered electron image

### $\text{Al}_2\text{O}_3\text{-TiB}_2$ composite

The thermal stability of this material is directly related to the oxidation of the dispersoid particles, which are present on the surface and/or connected to the surface through open porosity channels. The weight gain curves (Fig. 1b) indicate

diffusion-controlled kinetic, i.e. one-dimensional diffusion  $(DW/S)^2 \approx kt$ , at  $T = 700^\circ\text{C}$  and  $800^\circ\text{C}$ , and two-dimensional diffusion  $(1 - \alpha) \cdot \ln(1 - \alpha + \alpha) = kt$  (where  $\alpha$  is supposed equal to  $(DW/S)_t / (DW/S)_{\text{max}}$  and it is used as a mathematical artifice in order to define the kinetic relationship) at  $T \geq 900^\circ\text{C}$ . Actually the two-dimensional diffusion equation elaborated on the basis of a model for cylindrical particles can justifiably be proposed to explain the phenomenologies in our system, as it shows the development of needle-like and rod-shaped particles starting from  $700^\circ\text{C}$ , when the volume of the products is different from that of the reactants. Moreover, this second oxidation regime corresponds approximately to the temperature ( $\approx 900^\circ\text{C}$ ) that allows the formation of a continuous oxide scale.



**Fig. 6** Microstructure of the surfaces of  $\text{Si}_3\text{N}_4\text{-TiB}_2$  oxidized at  $1210^\circ\text{C}$ : *a*) morphology; *b*) back-scattered electron image

The oxidation curve  $T = 1100^\circ\text{C}$  presents a discontinuous trend around  $T = 200^\circ\text{C}$  that could be attributed to a changing in the oxidation mechanism from a parabolic behaviour to a linear one caused by the breaking of the continuous oxide scale formed during the initial stage of the oxidation reaction.



*Si<sub>3</sub>N<sub>4</sub>-TiB<sub>2</sub>*

From the analysis of the plots in Fig. 1c, three different oxidation regimes can be identified: at low ( $< \approx 1000^\circ\text{C}$ ), intermediate ( $\approx 1000 < T < \approx 1200^\circ\text{C}$ ) and high ( $> \approx 1200^\circ\text{C}$ ) temperature.

1) In the low-temperature range ( $< \approx 1000^\circ\text{C}$ ) the thermal stability of the composites does not involve  $\text{Si}_3\text{N}_4$ , therefore it is affected only by the reaction of  $\text{TiB}_2 \rightarrow \text{TiO}_2$ , with an evident bulking on every  $\text{TiB}_2$  starting particle (Fig. 4a). At  $T \approx 800^\circ\text{C}$  a more enhanced reaction of  $\text{TiB}_2$  to  $\text{TiO}_2$  rutile gives rise also to a further reaction of  $\text{TiO}_2$  with the secondary phase (Y-silicate) producing some  $\text{Y}_2\text{Ti}_2\text{O}_7$  needle like crystals as shown in back scattered electron image in Fig. 4b,  $\text{SiO}_2$  (from a slight oxidation of  $\text{Si}_3\text{N}_4$ ) also forms.

2) In the range  $\approx 1000 < T < \approx 1200^\circ\text{C}$ , the thermal stability of the composite is dependent on the oxidation of both the matrix and the second phase, particularly at  $T \approx 1100^\circ\text{C}$ . Weight gain against time could fit the parabolic law and it could stand for a fairly protective action of the oxide scale. The surface of the oxidized sample is completely covered by a scale of  $\text{TiO}_2$  crystals as shown in Fig. 5a. A large amount of  $\text{SiO}_2$  and  $\text{Y}_2\text{Ti}_2\text{O}_7$  form as a result of the oxidation of  $\text{Si}_3\text{N}_4$  and of the diffusion of Y from the bulk to the reaction interface [11]. The morphology of these oxidation products are highlight by the back-scattered image in Fig. 5b.

3) At  $T > \approx 1200^\circ\text{C}$ , weight gains after an initial parabolic stage tend to fit linear kinetics. Boric glassy phase forms in enhanced amounts and increases the

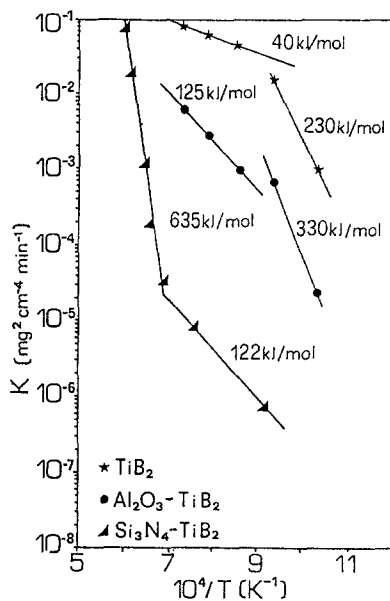


Fig. 7 Arrhenius plot of oxidation rate constants of  $\text{TiB}_2$ ,  $\text{Al}_2\text{O}_3\text{-TiB}_2$  and  $\text{Si}_3\text{N}_4\text{-TiB}_2$

oxidation rate of  $\text{Si}_3\text{N}_4$ . As the  $\text{Si}_3\text{N}_4$  matrix oxidizes, additional  $\text{TiB}_2$  particles are encountered and oxidized; these provide more boron to flux the  $\text{Si}_3\text{N}_4$  matrix. The fluid borosilicate glass allows oxygen to penetrate deeply into the body of the composite, which leads to additional attack of both  $\text{TiB}_2$  and  $\text{Si}_3\text{N}_4$ . The oxide scale at  $T > \approx 1200^\circ\text{C}$  does not protect the bulk from further oxidation and the linear kinetics are detected.

The Arrhenius plot of oxidation rate constants  $k$  against temperature are shown in Fig. 7.

For  $\text{TiB}_2$ , where diffusion-controlled mechanisms were found to be valid, the apparent activation energy is, at  $T < 900^\circ\text{C}$ ,  $E_a \approx 230$  kJ/mol and at  $T > 900^\circ\text{C}$ ,  $E_a \approx 40$  kJ/mol.

For  $\text{Al}_2\text{O}_3\text{-TiB}_2$ , at  $T < 900^\circ\text{C}$  (parabolic kinetics),  $E_a \approx 330$  kJ/mol and at  $T > 900^\circ\text{C}$ , (two-dimensional-diffusion regime),  $E_a \approx 125$  kJ/mol.

For  $\text{Si}_3\text{N}_4\text{-TiB}_2$ , the main feature is a net change in the slope at  $T \approx 1100^\circ\text{C}$  (the temperature at which oxidation of  $\text{Si}_3\text{N}_4$  is massive). At  $800 < T < 1100^\circ\text{C}$  the apparent activation energy  $E_a$  results  $\approx 120$  kJ/mol, a value that has been previously found for the diffusion of oxygen through silica or glassy silicates. In this case the diffusion of  $\text{O}_2$  or  $\text{N}_2$  through a complex layer (with  $\text{TiO}_2$ ,  $\text{SiO}_2$ ,  $\text{Y}_2\text{Ti}_2\text{O}_7$  and glassy silicates) could be proposed as the rate limiting process.

At  $T > \approx 1100^\circ\text{C}$ ,  $E_a$  results  $\approx 630$  kJ/mol, about the same value determined for the baseline  $\text{Si}_3\text{N}_4$  constituting the matrix of the composite [11]. With regard to this baseline silicon nitride, the diffusion of additives and impurities cations across the grain boundary phase channels to the reaction interface has been indicated as the governing step for oxidation [11]. In the case of the composites, an evident decrease in the oxidation resistance is associated with the presence of  $\text{TiB}_2$ . At temperatures  $> \approx 1100^\circ\text{C}$ , the compositional and microstructural characteristics of the surface of  $\text{Si}_3\text{N}_4\text{-TiB}_2$  composites result in a very complex system that makes the investigation of the reaction mechanisms difficult. They depend on the relative migration velocities of all the mobile participants across a particularly complex and inhomogeneous barrier layer and on the reactions that are sensitive to the local concentration of the various reacting species. Variation of thermodynamic parameters and oxidation products are associated with modification of the composition, the viscosity and morphology of the secondary phases and of the oxide scale.

## Conclusions

The use of thermogravimetric analysis for the weight change during oxidation of  $\text{TiB}_2$ , and of the composites  $\text{Al}_2\text{O}_3\text{-TiB}_2$  and  $\text{Si}_3\text{N}_4\text{-TiB}_2$ , combined with the analysis of the reaction products, allows the determination of kinetics and thermodynamic parameters of the process and the identification of the rate-control-

ling step. This can be used to suggest phenomenological models for the processes involved.

The oxidation of monolithic TiB<sub>2</sub> and of composites containing TiB<sub>2</sub> results in different behaviours and mechanisms depending on the temperature and time.

For TiB<sub>2</sub>:

1) In the range  $400^{\circ} \leq T \leq 900^{\circ}\text{C}$  and in the first stage of the oxidation at  $1000^{\circ}$  and  $1100^{\circ}\text{C}$ , the reaction is governed by a diffusion mechanism and crystalline TiO<sub>2</sub> and B<sub>2</sub>O<sub>3</sub> are detected on the oxide scale.

2) During isothermal treatments at  $1000^{\circ}$  and  $1100^{\circ}\text{C}$ , longer than 8 and 13 hours respectively, the increase in the active area for oxidation causes a mechanism governed by a linear law, the oxide scale being composed only of highly textured TiO<sub>2</sub> crystals.

For Al<sub>2</sub>O<sub>3</sub>-TiB<sub>2</sub>:

1) In the temperature range from about  $700^{\circ}$  to about  $900^{\circ}\text{C}$  a one-dimensional diffusion mechanism characterizes the rate governing step of the oxidation reaction. TiO<sub>2</sub> (rutile) and Al<sub>4</sub>B<sub>2</sub>O<sub>9</sub> are the crystalline phases observed on the oxidized surfaces.

2) At  $T > \approx 900^{\circ}\text{C}$  two-dimensional diffusion can be identified as the rate-governing step and the oxide scale is composed of highly oriented TiO<sub>2</sub> and Al<sub>18</sub>B<sub>4</sub>O<sub>33</sub>.

For Si<sub>3</sub>N<sub>4</sub>-TiB<sub>2</sub>:

1) Up to  $T \approx 1000^{\circ}\text{C}$  only the reaction of TiB<sub>2</sub> to TiO<sub>2</sub> and B<sub>2</sub>O<sub>3</sub> is observed.

2) At  $\approx 1000^{\circ} < T < \approx 1200^{\circ}\text{C}$  the rate limiting step could be the diffusion of O<sub>2</sub> or N<sub>2</sub> through a TiO<sub>2</sub>-rich silicatic layer.

3) At  $T > \approx 1200^{\circ}\text{C}$  a linear kinetic indicates the formation of a non-protective scale, which is very thick and whose morphology signifies a very fluid phase (may be a boric glass) that increases the oxidation rate of both TiB<sub>2</sub> and Si<sub>3</sub>N<sub>4</sub>.

## References

- 1 S. Baik and P. F. Becher, *J. Am. Ceram. Soc.*, 70 (1987) 527.
- 2 V. J. Tennery, C. B. Finch, C. S. Yust and G. W. Clark, Ed. by Viswanadham et al., Plenum, N. Y. 1983, p. 891-909.
- 3 A. Bellosi, T. Graziani, S. Guicciardi and A. Tampieri, 'Characteristics of TiB<sub>2</sub> Ceramics', presented at 9th Special Ceramics, London, December 1989, in print in the Proceedings
- 4 J. Matsushita, S. Hayashi and H. Saito, *J. Ceram. Soc. Jpn. Inter. Ed.*, 97 (1989) 1200.
- 5 I. Kimura, N. Hotta, Y. Hiraoka and N. Saito, *J. Europ. Ceram. Soc.*, 5 (1989) 23.
- 6 G. N. Babini, A. Bellosi and A. Fiegna, *Euro-Ceramics vol. 3*, G. Dewith, R. A. Terpstra, R. Metseelar eds. Elsevier Appl. Sci., 1989, p. 389.
- 7 A. Lebugle and G. Montel, *Rev. Int. Htes. Temp. et Refract.*, 11 (1974) 231.
- 8 G. R. Anstis, P. Chantikul, B. R. Lawn and D. B. Mashall, *J. Am. Ceram. Soc.* 64 (1981) 533.

- 9 A. Tampieri, A. Bellosi and V. Biasini, *Advanced Structural Inorganic Composites*, P. Vincenzini Ed., Elsevier Sci. Pub., B. V., 1991. pp. 408–420.
- 10 A. Bellosi, G. N. Babini 'Sintering and Characterization of Electroconductive  $\text{Al}_2\text{O}_3$ -based Composites', presented at the '4th International Symposium on Ceramic Materials & Components for Engines', Göteborg, June 10–12, 1991.
- 11 A. Bellosi and G. N. Babini, *Ceramic Materials and Components for Engines*, V. J. Tennerly Ed., Am. Ceram. Soc., (1989) 651.

**Zusammenfassung** — Im Hinblick auf die Neigung von  $\text{TiB}_2$  zur Oxidation wurde die thermische Stabilität von monolytischem  $\text{TiB}_2$  und der Gemische  $\text{Al}_2\text{O}_3$ -30Vol%  $\text{TiB}_2$  sowie  $\text{Si}_3\text{N}_4$ -20Vol%  $\text{TiB}_2$  untersucht. Die Temperatur, bei der  $\text{TiB}_2$  Keramik beginnt zu oxidieren, liegt bei  $400^\circ\text{C}$ , die Oxidationskinetik wird bis zu  $T=900^\circ\text{C}$  und im ersten Schritt der Oxidation bei  $1000^\circ$  bzw.  $1100^\circ\text{C}$  (bis zu 800 bzw. 500 min) durch Diffusion beherrscht, bei höheren Temperaturen und längeren Zeitabschnitten durch ein lineares Gesetz.

Eine Gewichtszunahme kann bei  $\text{Al}_2\text{O}_3$ - $\text{TiB}_2$ -Gemischen nur bei Temperaturen oberhalb etwa  $700^\circ\text{C}$  beobachtet werden und der geschwindigkeitsbestimmende Schritt der Oxidationsreaktion ist bei  $T=700^\circ\text{C}$  bzw.  $T=800^\circ\text{C}$  durch einen eindimensionalen, bei höheren Temperaturen durch einen zweidimensionalen Diffusionsmechanismus charakterisiert.

Bezüglich des  $\text{Si}_3\text{N}_4$ - $\text{TiB}_2$ -Gemisches wurden in Abhängigkeit von der Temperatur drei verschiedene Oxidationsverhalten beobachtet: bis etwa  $1000^\circ\text{C}$  betrifft die Reaktion nur die zweite Phase; bei Temperaturen zwischen  $1000^\circ$  und  $1200^\circ\text{C}$  wird die Diffusion von  $\text{O}_2$  oder  $\text{N}_2$  durch eine Oxidschicht als geschwindigkeitsbestimmender Schritt vorgeschlagen; bei Temperaturen oberhalb  $1200^\circ\text{C}$  zeigt eine lineare Kinetik die Bildung einer nichtschützenden dünnen Schicht